

Journal Pre-proof

Design of novel monoamine oxidase-B inhibitors based on piperine scaffold:
Structure-activity-toxicity, drug-likeness and efflux transport studies

Daniel Chavarria, Carlos Fernandes, Vera Silva, Cátia Silva, Eva Gil-Martins, Pedro Soares, Tiago Silva, Renata Silva, Fernando Remião, Paulo J. Oliveira, Fernanda Borges

PII: S0223-5234(19)30922-5

DOI: <https://doi.org/10.1016/j.ejmech.2019.111770>

Reference: EJMECH 111770

To appear in: *European Journal of Medicinal Chemistry*

Received Date: 18 August 2019

Revised Date: 6 October 2019

Accepted Date: 6 October 2019

Please cite this article as: D. Chavarria, C. Fernandes, V. Silva, Cá. Silva, E. Gil-Martins, P. Soares, T. Silva, R. Silva, F. Remião, P.J. Oliveira, F. Borges, Design of novel monoamine oxidase-B inhibitors based on piperine scaffold: Structure-activity-toxicity, drug-likeness and efflux transport studies, *European Journal of Medicinal Chemistry* (2019), doi: <https://doi.org/10.1016/j.ejmech.2019.111770>.

This is a PDF file of an article that has undergone enhancements after acceptance, such as the addition of a cover page and metadata, and formatting for readability, but it is not yet the definitive version of record. This version will undergo additional copyediting, typesetting and review before it is published in its final form, but we are providing this version to give early visibility of the article. Please note that, during the production process, errors may be discovered which could affect the content, and all legal disclaimers that apply to the journal pertain.

© 2019 Published by Elsevier Masson SAS.



Design of novel monoamine oxidase-B inhibitors based on piperine scaffold: structure-activity-toxicity, drug-likeness and efflux transport studies

Daniel Chavarria^{†1,2}, Carlos Fernandes^{†1}, Vera Silva^{1,3}, Cátia Silva¹, Eva Gil-Martins^{1,3}, Pedro Soares¹, Tiago Silva^{1,2}, Renata Silva³, Fernando Remião³, Paulo J. Oliveira², Fernanda Borges^{1*}

¹ CIQUP/Department of Chemistry and Biochemistry, Faculty of Sciences, University of Porto, Porto, Portugal

² CNC - Center for Neuroscience and Cell Biology, University of Coimbra, UC Biotech, Biocant Park, Cantanhede, Portugal.

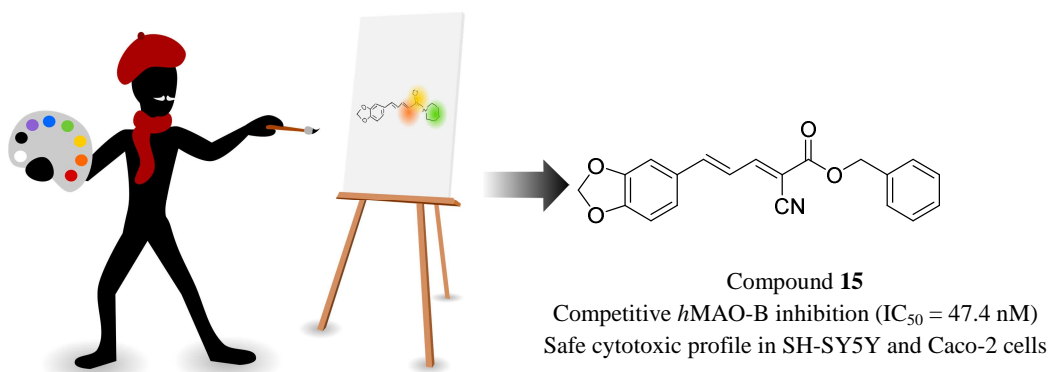
³ UCIBIO-REQUIMTE, Laboratory of Toxicology, Department of Biological Sciences, Faculty of Pharmacy, University of Porto, Porto, Portugal

† These authors contributed equally.

* Corresponding Authors:

Fernanda Borges, CIQUP/Department of Chemistry and Biochemistry, Faculty of Sciences, University of Porto, Porto 4169-007, Portugal. E-mail: fborges@fc.up.pt

Graphical abstract



Highlights

- A series of piperine derivatives was synthesized, eight of which acted as *h*MAO-B inhibitors.
- α -Cyano and benzyl ester substituents increased both potency and selectivity towards *h*MAO-B.
- Compounds **15** and **16** displayed slight P-gp inhibitory activity in Caco-2 cells.
- Compound **15** is highlighted as a potent, selective and competitive *h*MAO-B inhibitor.
- Compound **15** displayed favorable drug-like properties and a safe cytotoxic profile.

Abstract

Piperine has been associated with neuroprotective effects and monoamine oxidase (MAO) inhibition, thus being an attractive scaffold to develop new antiparkinsonian agents. Accordingly, we prepared a small library of piperine derivatives and screened the inhibitory activities towards human MAO isoforms (*h*MAO-A and *h*MAO-B). Structure-activity relationship (SAR) studies pointed out that the combination of α -cyano and benzyl ester groups increased both potency and selectivity towards *h*MAO-B. Kinetic experiments with compounds **7**, **10** and **15** indicated a competitive *h*MAO-B inhibition mechanism. Compounds **15** and **16**, at 10 μ M, caused a small but significant decrease in P-gp efflux activity in Caco-2 cells. Compound **15** stands out as the most potent piperine-based *h*MAO-B inhibitor ($IC_{50} = 47.4$ nM), displaying favorable drug-like properties and a broad safety window. Compound **15** is thus a suitable candidate for lead optimization and the development of multitarget-directed ligands.

Keywords: Parkinson's disease, Piperine, Monoamine oxidase, Cholinesterase, Structure-activity relationship.

Abbreviations: BBB: Blood-brain barrier; CHI: Chromatographic Hydrophobic Index; CNS: Central nervous system; DMAP: 4-(dimethylamino)pyridine; DCF: 2',7'-dichlorofluorescein; DCFH-DA: 2',7'-dichlorofluorescein diacetate; EDC: *N*-(3-dimethylaminopropyl)-*N'*-ethylcarbodiimide; HBA: hydrogen bond atom acceptor; HBD: hydrogen bond atom donor; K_m : Michaelis constant; K_i : inhibition constant; MAO: monoamine oxidase; MW: molecular weight; NR: neutral Red; PD: Parkinson's disease; P-gp: P-glycoprotein; PyBOP: benzotriazol-1-yl-oxytripyrrolidinophosphonium hexafluorophosphate; RB: rotatable bonds; RHO 123: Rhodamine 123; RS: reactive species; SAR: Structure-Activity Relationship; V_{max} : maximum velocity.

1. Introduction

Parkinson's disease (PD) is the second most common neurodegenerative disorder after Alzheimer's disease [1]. PD is characterized by the progressive and selective loss of dopaminergic neurons in the *substantia nigra* and by the presence of Lewy bodies [2], which decreases interstitial dopamine levels and leads to motor dysfunction [3, 4]. PD is also associated with non-motor symptoms such as cognitive decline, depression and sleep disorders, with some of them preceding the development of the classical motor symptoms [5, 6]. Current drug treatment of PD almost exclusively focuses on restoring the dopaminergic function and reducing the severity of motor handicap [7]. The main pharmacological approaches include dopamine replacement therapy with L-DOPA, inhibition of dopamine metabolism and reuptake, or the use of direct agonists of post-synaptic dopamine receptors [4, 7].

Monoamine oxidases (MAOs, EC 1.4.3.4) are flavin-dependent enzymes bound to the outer mitochondrial membrane [8]. Two MAO isoforms (MAO-A and MAO-B) may participate in the regulation of dopamine levels in neuronal tissue [9]. However, MAO-B is the main MAO isozyme involved in dopamine metabolism in parkinsonian brains, because MAO-B activity and expression are increased in most brain areas while MAO-A activity remains unchanged [10]. Selective irreversible MAO-B inhibitors, like selegiline and rasagiline, are used in PD monotherapy or in combination with dopamine precursor L-DOPA to reduce dopamine catabolism and thereby increase its half-life [11, 12]. More recently, safinamide, a reversible MAO-B inhibitor, was approved in the European Union to treat patients with mid- to late-stage PD [13].

Considering that the prevalence of PD is drastically increasing and no disease-modifying treatment emerged over the last few decades [14], great interest remains in the development of new antiparkinsonian drugs. Piperine (1-[5-(1,3-benzodioxol-5-yl)-1-oxo-2,4-pentadienyl]piperidine), compound **1**, **Figure 1**), the pungent component of several pepper species [15], presents several biological properties with potential therapeutic interest for PD. Piperine displayed antioxidant, anti-inflammatory and antiapoptotic activities in cultured neuronal cells [16] and in PD animal models [17-19]. Moreover, piperine was reported as a competitive, reversible and non-selective rMAO inhibitor [20]. Within this framework, we explored the piperine scaffold in a preliminary study, wherein the unequivocal structural elucidation of five piperine bioisosteres along with their *h*MAO inhibitory activities were assessed [21]. The data acquired put forward the significance of piperidinyl amide group to modulate the interaction of piperine derivatives with *h*MAOs [21].

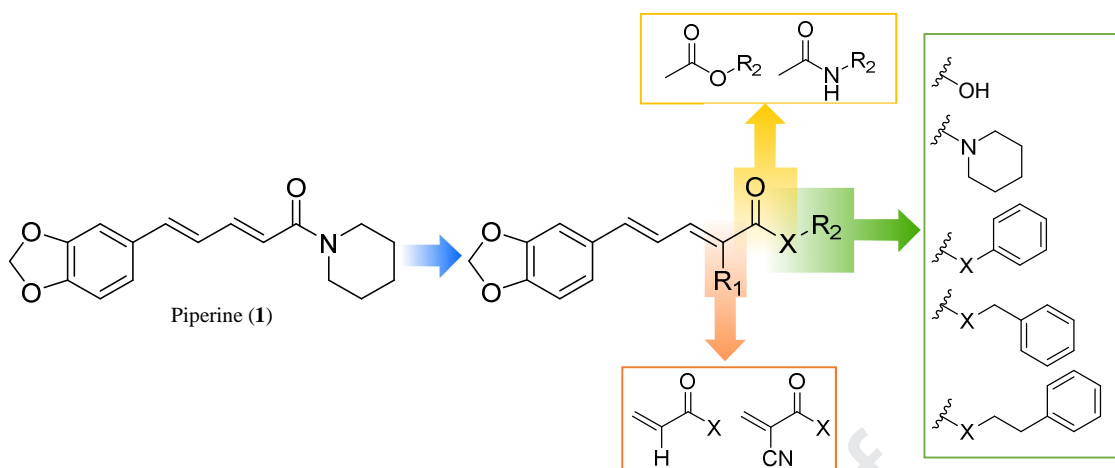


Figure 1. Rational design of the library based on piperine (compound **1**) scaffold.

- The promising results encouraged a second project aiming to identify the most favourable chemical modifications on the piperine scaffold required for the development of novel ligands with potential application in PD. Herein, we report the synthesis of a new library of piperine derivatives (Figure 1) and the establishment of new structure-activity-relationships (SAR). Following *h*MAO-B enzymatic and mechanistic studies, we investigated the cytotoxicity of the best inhibitors in two different human-derived cell lines (neuroblastoma cells (SH-SY5Y) and colon adenocarcinoma cells (Caco-2)). The compounds' ability to induce intracellular oxidative stress in SH-SY5Y cells and to modulate the P-glycoprotein (P-gp) activity by piperine derivatives in Caco-2 cells was also evaluated. Finally, we studied the drug-like properties of the best compounds. The compound's lipophilicity was evaluated by chromatographic hydrophobicity index (CHI).

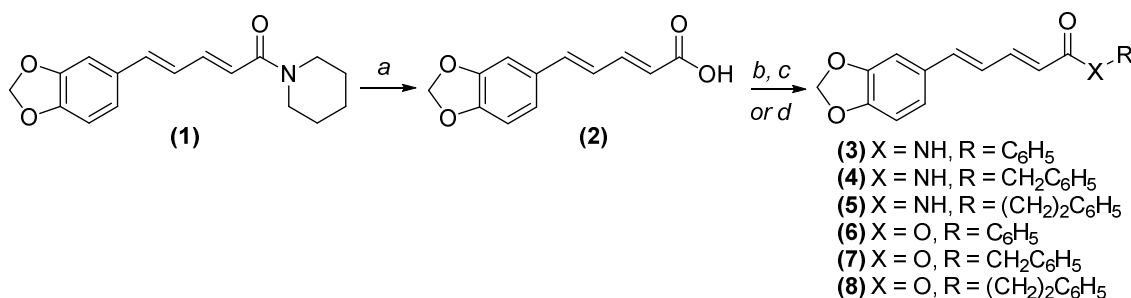
2. Results and discussion

2.1. Chemistry

Piperine-based compounds **2-16** were synthesized following the strategies represented in **Schemes 1** and **2**. Several modifications were performed at the diene tether and at the piperidiny amide group to attain structural diversity (**Figure 1**). Piperidiny moiety was removed to obtain free carboxylic acids or replaced by lipophilic groups (phenyl, benzyl or phenethyl) linked through ester or amide bonds. In addition, an α -cyano group was incorporated in the diene tether.

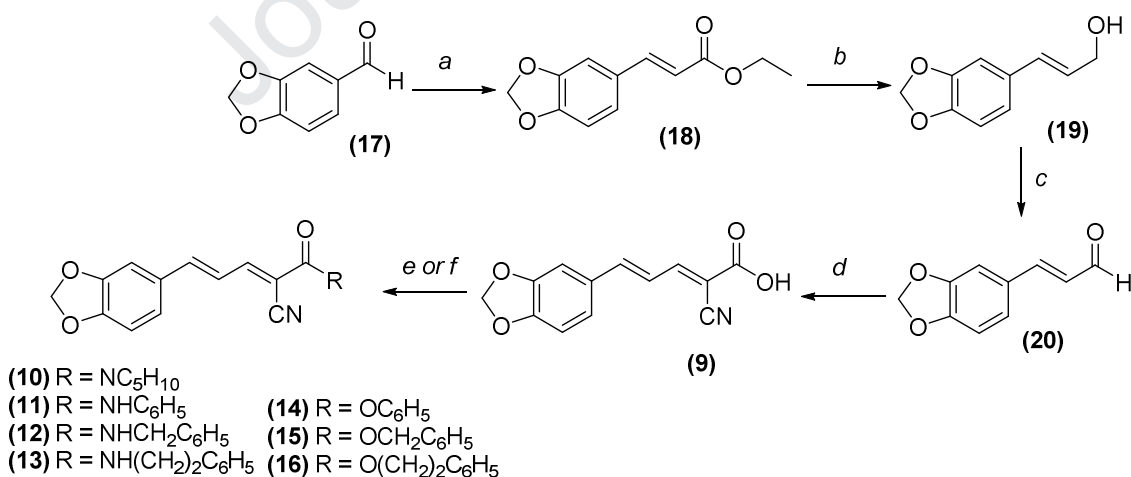
The hydrolysis of piperine in alkaline medium (**Scheme 1**, step *a*) yielded piperic acid (compound **2**, **Scheme 1**), which in turn reacted with the appropriate amines or alcohols to afford the corresponding amides **3-5** and esters **6-8**, respectively. Accordingly, amides **3-5** were synthesized via benzotriazol-1-yl-oxytripyrrolidinophosphonium hexafluorophosphate (PyBOP)-mediated amidation reaction, under alkaline conditions, between piperic acid and aniline, benzylamine or (2-bromoethyl)benzene (**Scheme 1**, step *b*). Piperic acid ester **6** was obtained by a Steglich esterification reaction, assisted by *N*-(3-dimethylaminopropyl)-*N'*-ethylcarbodiimide (EDC) and 4-

(dimethylamino)pyridine (DMAP), between piperic acid **2** and phenol (**Scheme 1**, step *c*). Esters **7** and **8** were synthesized from piperic acid **2** by bimolecular nucleophilic substitution with benzyl bromide and (2-bromoethyl)benzene, respectively (**Scheme 1**, step *d*).



Scheme 1. Synthetic strategy pursued to obtain piperine derivatives **2-8**. (a) Methanolic solution of NaOH 2 M, reflux, 24 h; (b) 1. DMF, DIPEA, PyBOP, CH₂Cl₂, 0 °C, 30 min; 2. Amine (aniline, benzylamine or (2-bromoethyl)benzene), rt, overnight; (c) 1. EDC.HCl, DMAP, CH₂Cl₂, rt, 30 min; 2. phenol, rt, overnight; (d) 1. K₂CO₃, DMF, rt, 30 min; 2. benzylbromide or (2-bromoethyl)benzene, 80 °C, 8 h.

The synthetic route used to obtain α -cyanopiperic acid (compound **9**) and derivatives **10-16** is shown in **Scheme 2**. The cinnamic derivative (compound **18**) used as starting material was prepared by a Knoevenagel-Doebner condensation between piperonal (compound **17**) and mono-ethyl malonate in pyridine and catalytic amounts of piperidine (**Scheme 2**, step *a*). The reduction of compound **18** with lithium aluminum hydride (LiAlH₄) afford the 3,4-methylenedioxcinnamyl alcohol (compound **19**) (**Scheme 2**, step *b*) that was subsequently oxidized to the 3,4-methylenedioxcinnamic aldehyde (compound **20**) with manganese dioxide (MnO₂) (**Scheme 2**, step *c*). α -Cyanopiperic acid (compound **9**) was obtained by a Knoevenagel condensation between compound **20** and cyanoacetic acid (**Scheme 2**, step *d*). Subsequent amidation (**Scheme 2**, step *e*) or Steglich esterification (**Scheme 2**, step *f*) reactions afforded compounds **10-16**.



Scheme 2. Synthetic strategy pursued to obtain α -CN derivatives **9-16**. (a) mono-ethyl malonate, pyridine, piperidine, 70 °C, 9 h; (b) 1. Argon atmosphere, dry THF, -78 °C, 30 min; 2. LiAlH₄, -78 °C to rt, 5 h; (c) MnO₂, CH₂Cl₂, rt, overnight; (d) cyanoacetic acid, pyridine, piperidine, 60 °C, 30 min; (e) 1. DMF, DIPEA, PyBOP, CH₂Cl₂, 0 °C, 30 min; 2. Amine (aniline, benzylamine or (2-bromoethyl)benzene), rt, overnight; (f) 1. EDC.HCl, DMAP, CH₂Cl₂, rt, 30 min; 2. Phenol, benzyl alcohol or 2-phenylethanol, rt, overnight.

2.2. Monoamine oxidase inhibition studies

The potential effects of piperine and its analogues (compounds **1-16**) on *h*MAOs activity were studied by spectrophotometry, using kynuramine as substrate and recombinant *h*MAO-A and -B isoforms [21, 22]. The *h*MAO-A and *h*MAO-B inhibitory potency (IC_{50}) and selectivity (SI) data obtained with the compounds under study and standard inhibitors (clorgyline for *h*MAO-A and (*R*)-(-)-deprenyl, rasagiline, safinamide for *h*MAO-B) are reported in **Table 1**.

Table 1. *h*MAO inhibitory activities of compounds **1-16** and standard inhibitors.

	R	Compound	IC_{50} (μ M)		SI ^b
			<i>h</i> MAO-A	<i>h</i> MAO-B	
		2^e	— ^a	— ^a	—
		1^e	— ^a	1.05±0.08	10 ^d
		3^e	— ^a	— ^a	—
		4^e	— ^a	— ^a	—
		5	— ^a	— ^a	—
		6^e	— ^c	0.156±0.008	> 64 ^d
		7^e	4.24±0.56	0.167±0.011	25
		8	— ^a	0.448±0.043	> 22 ^d
		9	— ^a	— ^a	—
		10	— ^a	0.143±0.080	> 70 ^d
		11	— ^a	— ^a	—
		12	— ^a	0.471±0.008	> 21 ^d
		13	— ^a	— ^a	—
		14	— ^a	0.215±0.038	>47 ^d
		15	— ^a	0.0474±0.0042	> 211 ^d
		16	— ^a	0.0992±0.0082	> 101 ^d
	(<i>R</i>)-(-)-Deprenyl ^e	—	20.1±1.9	0.0386±0.0043	522
	Rasagiline	—	3.65±0.31	147.3±249	24
	Safinamide	—	— ^a	0.0231±0.0026	> 433 ^d
	Clorgyline ^e	—	0.00274±0.00047	2.21±0.26	0.00124

^a Inactive at 10 μ M;

^b SI: *h*MAO-B selectivity index = $IC_{50}(hMAO-A)/IC_{50}(hMAO-B)$.

^c Not soluble in phosphate buffer at concentrations higher than 10 μ M.

^d Values obtained under the assumption that the corresponding IC₅₀ value against *h*MAO-A or *h*MAO-B is the highest concentration tested (10 μM).

^e Data from Chavarria *et al.* [21].

2.2.1. Structure-activity relationship studies

The results obtained show that the compounds that presented *h*MAOs inhibitory activity were more selective towards the isoform B. As previously reported, piperine displayed moderate and selective inhibition towards *h*MAO-B (compound **1**, IC₅₀ = 1.05 μM, SI = 10) in our experimental conditions [21]. Interestingly, the introduction of an α-CN group at the diene tether improved the *h*MAO-B inhibitory activity (compound **10**: IC₅₀ = 143 nM).

Compounds containing a piperidinyl amide moiety were active towards *h*MAO-B (compounds **1** and **10**). The replacement of the piperidinyl group by a carboxylic acid (compounds **2** and **9**) completely abolished *h*MAO inhibition. Primary amides were also unable to inhibit both *h*MAO isoforms (compounds **3-5**, **11** and **13**) or have modest inhibitory activity towards *h*MAO-B (compounds **12**). On the other hand, except for compound **14**, esters **6-8**, **15** and **16** were more potent and selective *h*MAO-B inhibitors than piperidinyl derivatives **1** and **14**.

Concerning ester and primary amide substituents, benzyl derivatives displayed the most promising results. Piperic acid benzyl ester presented an IC₅₀ value similar to that of the phenyl derivative and lower than the phenethyl analogue (compound **7**: IC₅₀ = 167 nM; compound **6**: IC₅₀ = 156 nM; compound **8**: IC₅₀ = 448 nM). All α-cyanobenzyl derivatives acted as *h*MAO-B inhibitors. Compound **12** was the only primary amide of α-cyanopiperic acid acting as *h*MAO-B inhibitor (compound **12**: IC₅₀ = 471 nM). Benzyl ester **15** was more active than phenethyl ester **16**, which in turn was more potent than phenyl ester **14** (compound **15**: IC₅₀ = 47.4 nM; compound **16**: IC₅₀ = 99.2 nM; compound **14**: IC₅₀ = 215 nM). Therefore, we concluded that the combination of the benzyl group with a cyano group enhanced the *h*MAO-B inhibitory properties.

In fact, with the exception of compound **14**, compounds containing an α-CN presented lower IC₅₀ values towards *h*MAO-B than their unsubstituted counterparts, without showing significant *h*MAO-A inhibitory activity at 10 μM. This chemical modification also influenced the selectivity of the compounds. The SI of compounds **10**, **15** and **16** were 5 to 8.4-fold higher than that of piperine and compounds **7** and **8** (compound **1** [SI = 10] *vs* compound **10** [SI = 70]; compound **7** [SI = 25] *vs* compound **15** [SI = 211]; compound **8** [SI = 22] *vs* compound **16** [SI = 101]). Compound **15** showed the lowest IC₅₀ value towards *h*MAO-B and the highest *h*MAO-B SI (compound **15**: IC₅₀ = 47.4 nM; SI = 211).

2.2.2. Evaluation of human monoamine oxidase-B inhibition mechanism

To further investigate the *h*MAO-B inhibition mechanism of the best *h*MAO-B inhibitor (compound **15**), kinetic experiments were performed. The study was extended to compounds **7** and **10** to evaluate the influence of the α-CN or piperidinyl amide groups in the enzyme inhibition mechanisms. We measured the initial rates of the *h*MAO-catalyzed deamination of six different concentrations of kynuramine in the absence or presence of three different concentrations of the inhibitors. The results obtained are depicted in **Figure 2**. Kinetic parameters of Michaelis-Menten reaction (Michaelis constant,

K_m , and maximum velocity, V_{max}) were determined by the graphical analysis of the double reciprocal Lineweaver-Burk plots. The presence of increasing concentrations of compounds **7**, **10** and **15** resulted in an increase of K_m values and a maintenance of V_{max} . The Lineweaver-Burk plots (**Figures 2A-C**) of these compounds remained linear and intersected at the y-axis. These observations indicate that the piperine derivatives **7**, **10** and **15** act as competitive inhibitors.

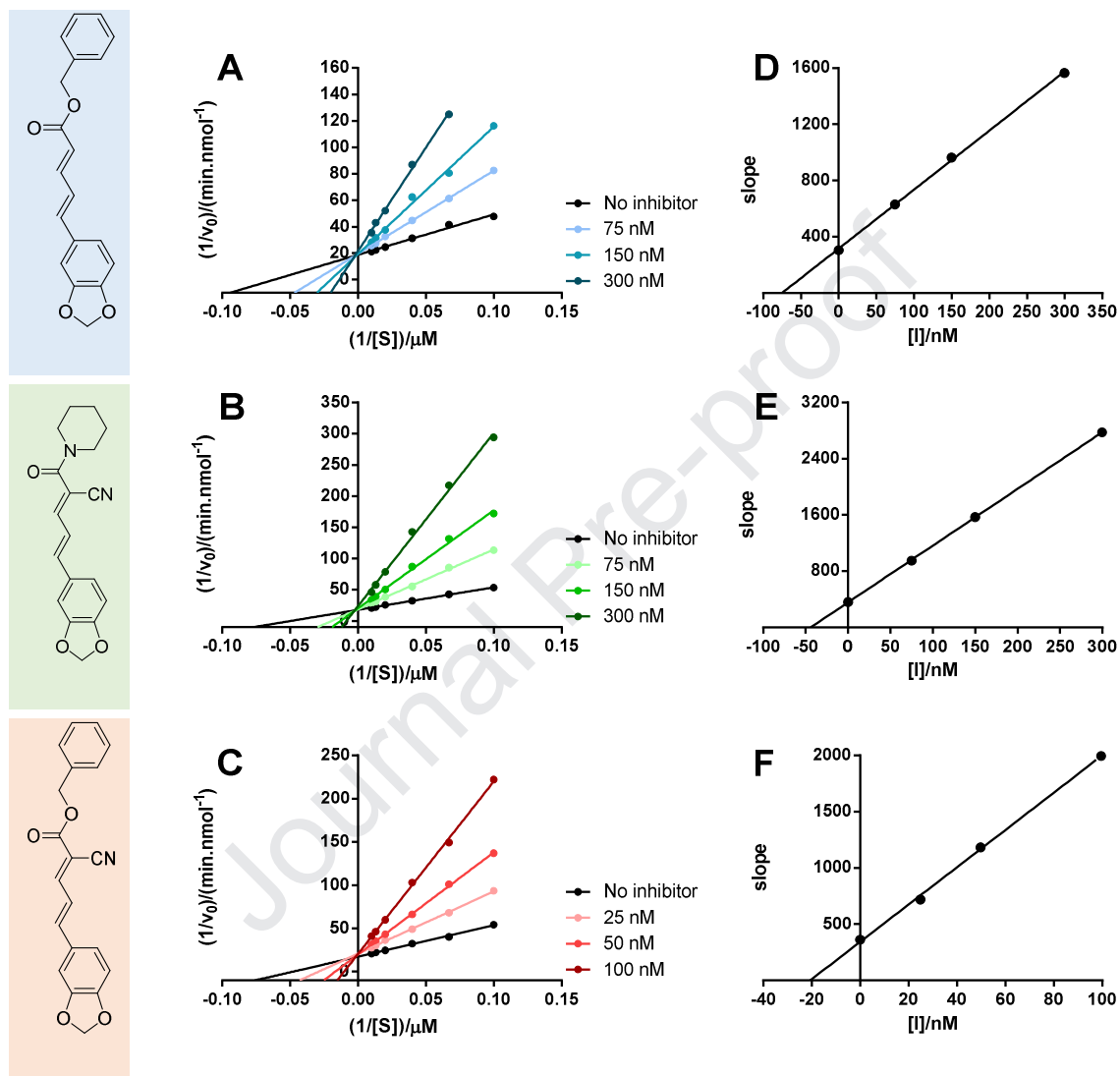


Figure 2. Kinetic studies on the mechanism of *h*MAO-B inhibition by compounds **7** (**A** and **D**), **10** (**B** and **E**) and **15** (**C** and **F**). (**A-C**) Double reciprocal plots of the initial velocity of *h*MAO-B at increasing substrate concentrations (10-100 μ M) in the absence or the presence of the inhibitor. (**D-F**) Secondary plots of the slope of each Lineweaver-Burk (K_m/V_{max}) versus the inhibitor concentration.

The data obtained from the Lineweaver-Burk were then replotted as the slope against the inhibitor concentrations to obtain the inhibition constants (K_i) of the mentioned compounds. The x-axis intercept is $-K_i$ (**Figures 2D-F**). Compounds **7**, **10** and **15** displayed K_i values of 75.0 nM, 20.6 nM and 44.1 nM, respectively. The estimated K_i values were well correlated with the inhibition mechanism established from the kinetic experiments.

2.3. Cellular studies

2.3.1. Evaluation of cytotoxicity profile

To study the cytotoxicity profile of the most promising piperine-based compounds (*h*MAO-B $IC_{50} < 200$ nM), we performed cellular cytotoxicity assays in differentiated neuroblastoma (SH-SY5Y) cells and in colon adenocarcinoma (Caco-2) cells. SH-SY5Y and Caco-2 cells are commonly used to evaluate the safety of drug candidates [23, 24]. In this study, SH-SY5Y cells were treated with a differentiation-inducing agent to obtain cells morphologically similar to mature dopaminergic neurons [25]. Considering that PD mainly affects dopaminergic neurons [26], differentiated SH-SY5Y cells are a suitable *in vitro* model to study the neurotoxicity of drug candidates with potential application in PD [27].

Differentiated SH-SY5Y cells and Caco-2 cells were incubated with two different concentrations (10 and 50 μ M) of compounds **6**, **7**, **10**, **15** and **16** for 24 h. Piperine (compound **1**) was also tested to study the effect of the structural modification of piperine scaffold on the cytotoxicity profile of compounds. Cellular cytotoxicity was evaluated using the resazurin reduction assay, which estimates the metabolic activity of viable cells [28], and the neutral red (NR) uptake assay, which relies on the lysosomal accumulation of the dye NR in living cells [29]. The results are presented in **Figure 3** and expressed as mean (% of control) \pm SEM of three independent experiments ($n = 3$).

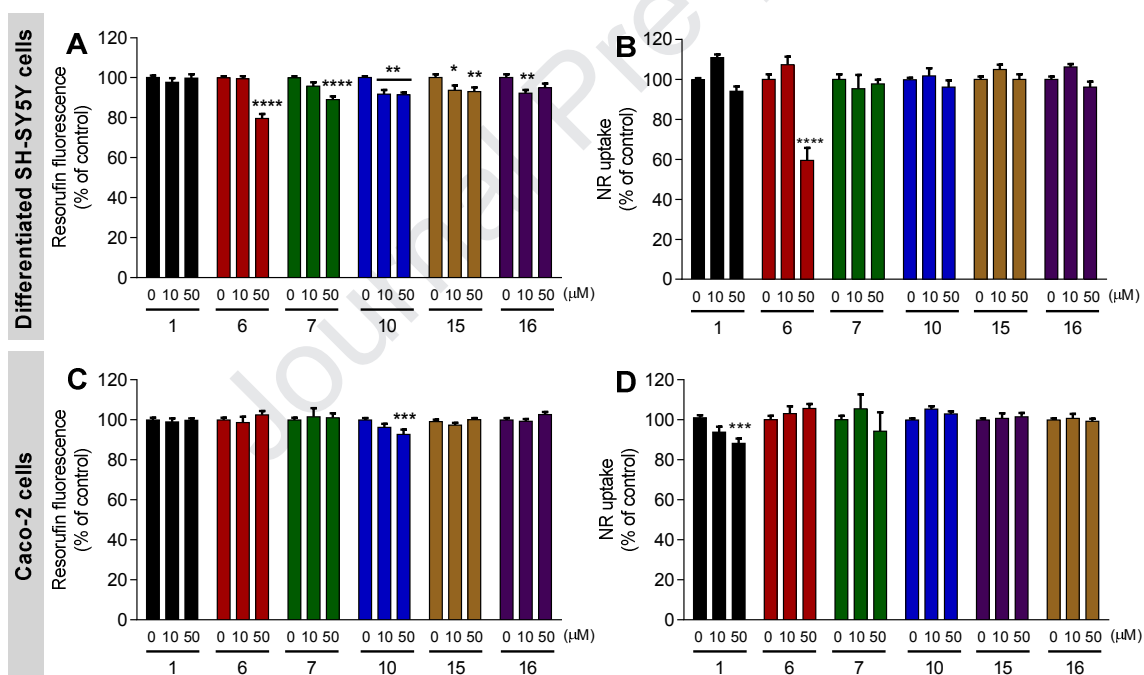


Figure 3. Cellular viability of differentiated SH-SY5Y cells (**A-B**) and Caco-2 cells (**C-D**) after incubation with piperine (**1**) and compounds **6**, **7**, **10**, **15** and **16** at two different concentrations (10 μ M and 50 μ M) for 24 h. Cellular viability was evaluated by measuring metabolic (**A** and **C**) and lysosomal activities (**B** and **D**) using the resazurin reduction assay and the neutral red uptake assay, respectively. Statistical comparisons were performed using the parametric method of two-way ANOVA, followed by the Dunnett's multiple comparisons test. In all cases, p values lower than 0.05 were considered significant (* $p < 0.05$, ** $p < 0.01$, *** $p < 0.001$, **** $p < 0.0001$ vs untreated cells).

The results obtained show that the treatment of differentiated SH-SY5Y cells with compounds **1**, **7**, **10**, **15** and **16** did not markedly decrease the resazurin reduction or the NR uptake when compared to

control cells (% resazurin reduction and NR uptake were always > 85 %) (**Figure 3A** and **3B**). However, treatment with compound **6** at the highest tested concentration (50 μ M) led to significant reductions in both resorufin fluorescence (79.7 ± 2.1 %, $p < 0.0001$, **Figure 3A**) and in NR uptake (59.4 ± 6.5 %, $p < 0.0001$, **Figure 3B**). In addition, both cellular metabolic and lysosomal activities in Caco-2 cells (**Figures 3C** and **3D**, respectively) were not markedly affected by the treatment with any of the tested piperine derivatives.

Overall, the acquired data suggest that piperine derivatives **7**, **10**, **15** and **16** present a safe cytotoxicity profile in both human-derived neuroblastoma and adenocarcinoma cells (% resazurin reduction and NR uptake were always > 85 %).

2.3.2. Evaluation of intracellular oxidative stress

The toxicity of numerous xenobiotics may be linked to the increased levels of oxidative stress, which are largely related to the formation of reactive species (RS) [30]. Therefore, we evaluated the intracellular oxidative stress levels in differentiated SH-SY5Y cells. After exposing the cells to piperine (compound **1**) and compounds **6**, **7**, **10**, **15** and **16** at two different concentrations (10 and 50 μ M) for 24 h, the intracellular RS levels were measured using the 2',7'-dichlorofluorescein diacetate (DCFH-DA) method. The results are expressed as 2',7'-dichlorofluorescein (DCF) fluorescence (% of control) \pm SEM ($n = 3$) and are depicted in **Figure 4**.

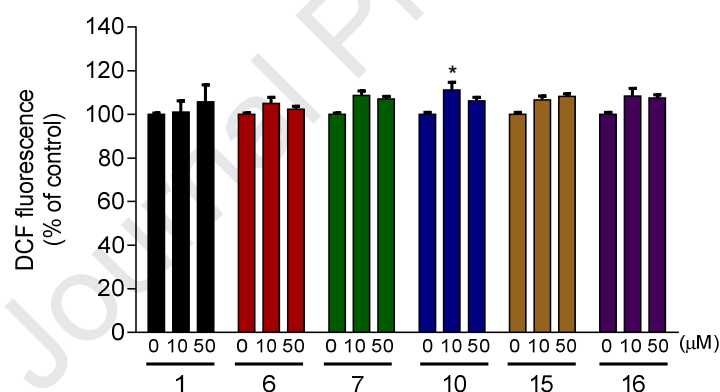


Figure 4. Evaluation of intracellular oxidative stress levels in differentiated SH-SY5Y cells evaluated by the DCF fluorescence assay, after treatment with piperine (compound **1**) and compounds **6**, **7**, **10** and **15** and **16** at two different concentrations (10 μ M and 50 μ M) for 24 h. Results are expressed as DCF fluorescence (% of control) \pm SEM ($n = 3$). Statistical comparisons were performed using the parametric method of two-way ANOVA, followed by the Dunnett's multiple comparisons test.

Among the tested piperine derivatives, only compound **10** led to a slight but significant increase in DCF fluorescence (111.1 ± 3.5 %, $p < 0.5$) when compared to non-treated cells (**Figure 4**). Given that compound **10** did not exhibit cytotoxicity at the tested concentrations (**Figures 3A** and **3B**), the results obtained suggest that the slightly increased RS levels did not inflict oxidative damage in SH-SY5Y cells.

2.3.3. Evaluation of P-glycoprotein (P-gp) transport activity

The delivery of therapeutic agents into the brain is strongly hampered by the blood-brain barrier (BBB) [31]. In fact, more than 98 % of all small drugs are unable to cross the BBB [32]. An important

gatekeeper of the BBB is P-gp, an ATP-driven efflux pump localized in the luminal membrane of brain capillary endothelial cells [33]. P-glycoprotein restricts the access of a large number of prescribed drugs to the central nervous system (CNS) and contributes to the poor success rates of CNS drug candidates [33].

Considering that P-gp is highly expressed in Caco-2 cells, this cellular model is widely used not only to screen the P-gp-mediated transport of drugs [34], but also to evaluate the influence of new drug candidates in P-gp expression and/or activity [35, 36]. In addition, Caco-2 cells are commonly used as a surrogate BBB model to study drug permeation [37-39].

We evaluated the P-gp modulatory activity of piperine (compound **1**) and compounds **7**, **10**, **15** and **16** in Caco-2 cells, using Rhodamine 123 (RHO 123) as a P-gp substrate and zosuquidar as a specific third-generation P-gp inhibitor [40]. Increased P-gp activity enhances RHO 123 efflux, leading to a decrease in the intracellular fluorescence intensity under normal conditions (FI_{NA}). Therefore, the RHO 123 accumulation ratio (FI_{IA}/FI_{NA}) will be higher than the control experiments (see supplementary information, **Equation S3**). On the other hand, lower P-gp activity is associated with higher FI_{NA} , as a result of the decreased RHO 123 efflux and consequent increase of RHO 123 intracellular accumulation. Thus, the FI_{IA}/FI_{NA} ratio will be lower than the control experiments (see supplementary information, **Equation S3**).

The results presented in **Figure 5** show that compounds **10**, **15** and **16**, at 10 μ M, significantly affected the intracellular accumulation of RHO 123, resulting in significant differences in P-gp transport activity. On the other hand, piperine (compound **1**) and compound **7** did not significantly change P-gp-mediated RHO 123 efflux.

Compound **10** significantly increased P-gp activity in a short-incubation period, resulting in a decreased RHO123 accumulation and, consequently, in a higher FI_{IA}/FI_{NA} ratio. Therefore, compound **10** demonstrated potential for P-gp activation. Given the short incubation period with both the P-gp substrate and the test compounds, the effect observed with compound **10** did not reflect the potential contribution of an increased protein expression. (**Figure 5**).

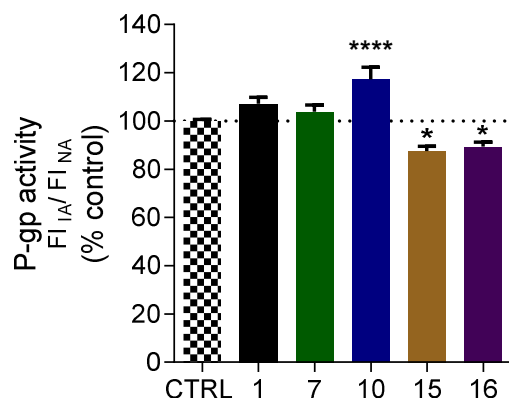


Figure 5. Evaluation of P-gp activity by fluorescence spectroscopy in Caco-2 cells exposed to compounds **1**, **7**, **10**, **15** and **16** (10 μ M) only during the incubation period with the fluorescent substrate (RHO 123, 5 μ M). Results are presented as mean \pm SEM from at least three independent experiments, performed in triplicate. Statistical

comparisons were made using the parametric method of one-way ANOVA, followed by the Dunnett's multiple comparisons test (**** $p < 0.0001$ vs. control cells).

Piperine derivatives **15** and **16**, at 10 μM , significantly reduced RHO 123 efflux, resulting in a decreased $\text{FI}_{\text{IA}}/\text{FI}_{\text{NA}}$ ratio that indicates mild P-gp inhibition. Together with the data obtained in *h*MAO inhibition studies, these findings show that compounds **15** and **16** are potent *h*MAO-B inhibitors with mild P-gp inhibitory activity.

Mild P-gp inhibition can be advantageous in combination therapy of PD. Since several antiparkinsonian agents such as L-DOPA are P-gp substrates [41], mild P-gp inhibition may decrease the drug efflux at the BBB, improve the drug delivery into the CNS and provide a longer symptomatic relief [42].

2.4. Evaluation of drug-like properties

We studied drug-like properties of piperine and the most promising *h*MAO-B inhibitors (compounds **7**, **15** and **16**) to predict their ability to attain the CNS. Compound **10** was excluded because it presented a positive modulatory effect on P-gp (**Figure 5**).

First, we determined the chromatographic hydrophobic index $\log D$ at pH 7.4 ($\text{CHI } \log D_{7.4}$), a parameter used to assess the compounds' hydrophobicity [43, 44]. Overall, the tested compounds presented $\text{CHI } \log D_{7.4}$ values between 2.4 and 3.8 (**Table 2**). Compounds **7**, **15** and **16** displayed higher CHI values than piperine. These results indicate an increase in lipophilicity with the replacement of the piperidinyl ring by benzyl or phenethyl ester groups.

Table 2. Retention times (t_{R}) obtained by LC/UV at pH 7.4 and calculated CHI and $\text{CHI } \log D_{7.4}$ parameters of compounds **1**, **7**, **15** and **16**

Compound	t_{R} (min)	CHI^a	$\text{CHI } \log D_{7.4}^b$
1	10.61	73.45	2.39
7	12.46	102.14	3.90
15	12.11	96.73	3.61
16	12.37	100.75	3.82

^a CHI values were calculated using the equation obtained in the linear correlation (see supplementary information, **Figure S1**).

^b $\text{CHI } \log D_{7.4}$ were back-calculated using the equation $\text{CHI } \log D_{7.4} = (0.0525 \times \text{CHI}) - 1.467$.

Other physicochemical properties were also estimated. These included molecular weight (MW), topological polar surface area (TPSA in \AA), number of hydrogen acceptors (HBA), number of hydrogen donors (HBD) and number of rotatable bonds (RB). The values obtained were in line with the reported limits of CNS-active drugs (**Table 3**). Another parameter used to assess the ability of a molecule to cross the BBB by passive diffusion is the logarithm of the ratio of the concentration of the compound in the brain and in the blood ($\log \text{BB}$). Compounds with $\log \text{BB} < -1$ have low distribution into the brain and thus are unlikely to act as CNS drugs [45]. Piperine and compounds **7**, **15** and **16** showed estimated $\log \text{BB}$ values above -1 suggesting that they may be able to cross the BBB and reach the CNS (**Table 3**).

Table 3. Predicted drug-like properties of piperine and compounds **7**, **10**, **15** and **16**.

Compound	MW ^a	TPSA ^a	HBA ^a	HBD ^a	RB ^a	logBB ^a
1	285.3	38.77	3	0	4	-0.185
7	308.3	44.76	4	0	6	0.059
15	333.3	68.55	5	0	6	-0.194
16	347.4	68.55	5	0	7	-0.175
CNS ⁺ drugs	< 500 ^[46]	< 90 ^[46]	< 7 ^[47]	< 3 ^[47]	< 8 ^[47]	≥ -1 ^[45]

^a Properties predicted using the Stardrop software. MW: molecular weight; TPSA: topological polar surface area; HBA: number of H-bond acceptor atoms; HBD: number of H-bond donor atoms; RB: number of rotatable bonds; logBB: logarithm of the ratio of the concentration of a drug in the brain and in the blood.

3. Conclusion

We successfully obtained a small library of piperine derivatives and explored their inhibitory activities towards *h*MAO-A and *h*MAO-B. Piperine and derivatives thereof displayed selective *h*MAO-B inhibition. SAR studies indicated that the presence of an α -cyano group increase *h*MAO-B inhibitory properties and that ester derivatives were considerably more active towards *h*MAO-B than amides and carboxylic acids. Concerning the lipophilic group bound to the ester/amide function, benzyl derivatives were the most potent *h*MAO-B inhibitors, followed by phenethyl and phenyl derivatives. Remarkably, the combination of an α -cyano group with ester groups enhanced *h*MAO-B inhibition potency and selectivity, leading to an up to 22-fold decrease of *h*MAO-B IC₅₀ values in comparison to piperine (**1**). Compounds **6**, **7**, **10**, **15** and **16** were the most potent *h*MAO-B inhibitors, with IC₅₀ values within the nanomolar range. Kinetic studies indicated that the piperine derivatives operated via a competitive inhibition mechanism. In general, piperine and compounds **7**, **10**, **15** and **16** presented safe cytotoxicity profiles in human-derived neuroblastoma and colon adenocarcinoma cells. Small decreases of FI_{IA}/FI_{NA} ratios associated with increased intracellular RHO 123 accumulation in Caco-2 cells were also observed for compounds **15** and **16** at 10 μ M, indicating a slight P-gp inhibition.

Compound **15** stands out as a non-cytotoxic, potent and selective *h*MAO-B inhibitor (IC₅₀ = 47.4 nM, SI = 211) with small P-gp inhibitory activity and suitable physicochemical properties for BBB permeation. Therefore, compound **15** is a valid candidate for lead optimization. In this context, the modification of the benzyl ester group or the benzodioxole ring can be looked as a valid strategy to obtain new molecules with improved efficacy and potency. Considering that PD and other neurodegenerative diseases result from the interplay between multiple pathological mechanisms, compound **15** can also be fused or merged with other neuroprotective agents to obtain drug candidates with a polypharmacological profile.

4. Experimental section

4.1. Synthesis of piperine derivatives

4.1.1. Synthesis of (2*E*,4*E*)-5-(benzo[*d*][1,3]dioxol-5-yl)penta-2,4-dienoic acid (2**).** Synthesis and structural analysis were previously reported [21].

4.1.2. General procedure for the synthesis of amides. Piperic acid **2** or cyanopiperic acid **9** (1 mmol) were dissolved in DMF and DIPEA (1.01 mmol). The mixture was cooled at 0 °C on an ice bath, and a solution of PyBOP (1.01 mmol) in dichloromethane was slowly added. The mixture was stirred for 30 min, and the appropriate amine (phenyl amine, benzyl amine or phenethyl amine) (1.01 mmol) was added. The mixture was stirred overnight at room temperature. Purification conditions are described in literature [21, 48]. In the cases that different conditions were used they were reported.

(2E,4E)-5-(benzo[d][1,3]dioxol-5-yl)-N-phenylpenta-2,4-dienamide (3). Synthesis and structural analysis were previously reported [21].

(2E,4E)-5-(benzo[d][1,3]dioxol-5-yl)-N-benzylpenta-2,4-dienamide (4). Synthesis and structural analysis were previously reported [21].

(2E,4E)-5-(benzo[d][1,3]dioxol-5-yl)-N-phenethylpenta-2,4-dienamide (5). $\eta = 82\%$. ^1H NMR (CDCl_3-d_1): δ (ppm) = 2.87 (*t*, $J = 6.9$ Hz, 2H, $\text{NHCH}_2\text{CH}_2\text{Ph}$), 3.62 (*m*, 2H, $\text{NHCH}_2\text{CH}_2\text{Ph}$), 5.54 (*t*, $J = 5.4$ Hz, 1H, NH), 5.84 (*d*, $J = 14.9$ Hz, 1H, $\text{H}\alpha$), 5.97 (*s*, 2H, OCH_2O), 6.65 (*dd*, $J = 11.0$ Hz, 15.2 Hz, 1H, $\text{H}\gamma$), 6.76 (*m*, 2H, H5 , $\text{H}\delta$), 6.88 (*dd*, $J = 1.6$ Hz, 8.1 Hz, 1H, H6), 6.90 (*d*, $J = 1.6$ Hz, 1H, H2), 7.23 (*m*, 3H, $\text{H3}'$, $\text{H4}'$, $\text{H5}'$), 7.33 (*m*, 3H, $\text{H2}'$, $\text{H6}'$, $\text{H}\beta$). ^{13}C NMR (CDCl_3-d_1): δ (ppm) = 37.7 ($\text{NHCH}_2\text{CH}_2\text{Ph}$), 40.7 ($\text{NHCH}_2\text{CH}_2\text{Ph}$), 101.3 (OCH_2O), 105.7 (C2), 108.5 (C5), 122.6 (C α), 123.0 (C6), 124.6 (C γ), 126.5 (C4'), 128.7 (C2', C6'), 128.8 (C3', C5'), 130.9 (C1), 139.0 (C δ , C1'), 141.1 (C β), 148.2 (C3), 148.3 (C4), 166.0 (CONH). EI/MS m/z (%): 321.2 (M^{*+} , 48), 201.1 (100), 143.1 (19), 115.1 (73), 96.1 (26).

(2E,4E)-5-(benzo[d][1,3]dioxol-5-yl)-2-(piperidine-1-carbonyl)penta-2,4-dienitrile (10). $\eta = 70\%$. ^1H NMR ($\text{DMSO}-d_6$): δ (ppm) = 1.54 (*m*, 4H, $\text{NCH}_2\text{CH}_2\text{CH}_2$), 1.65 (*m*, 2H, $\text{NCH}_2\text{CH}_2\text{CH}_2$), 4.00 (*m*, 4H, $\text{NCH}_2\text{CH}_2\text{CH}_2$), 6.10 (*s*, 2H, OCH_2O), 6.98 (*d*, $J = 8.2$ Hz, 1H, H5), 7.03 (*dd*, $J = 11.4$ Hz, 15.2 Hz, 1H, $\text{H}\gamma$), 7.13 (*dd*, $J = 1.5$ Hz, 8.1 Hz, 1H, H6), 7.34 (*m*, 2H, H2 , $\text{H}\delta$), 7.55 (*d*, $J = 11.4$ Hz, 1H, $\text{H}\beta$). ^{13}C NMR ($\text{DMSO}-d_6$): δ (ppm) = 24.3 ($\text{NCH}_2\text{CH}_2\text{CH}_2$), 25.9 ($\text{NCH}_2\text{CH}_2\text{CH}_2$, $\text{NCH}_2\text{CH}_2\text{CH}_2$), 102.2 (OCH_2O), 105.8 (C α), 106.9 (C2), 109.2 (C5), 116.0 (CN), 121.7 (C6), 125.2 (C γ), 130.0 (C1), 146.2 (C δ), 148.7 (C3), 149.9 (C4), 152.0 (C β), 162.3 (CON). EI/MS m/z (%): 310.1 (M^{*+} , 88), 225.0 (81), 197.0 (65), 159.0 (40), 140.0 (100), 113.0 (30), 84 (32).

(2E,4E)-5-(benzo[d][1,3]dioxol-5-yl)-2-cyano-N-phenylpenta-2,4-dienamide (11). The crude product was purified by flash column chromatography (silica gel, dichloromethane). $\eta = 44\%$. ^1H NMR (DMSO- d_6): δ (ppm) = 6.12 (s, 2H, OCH₂O), 7.01 (d, $J = 8.1$ Hz, 1H, H5), 7.12 (m, 2H, H γ , H δ), 7.22 (dd, $J = 1.6$ Hz, 8.2 Hz, 1H, H6), 7.35 (m, 2H, H2, H4'), 7.43 (m, 2H, H3', H5'), 7.66 (m, 2H, H2', H6'), 10.18 (s, 1H, NH). ^{13}C NMR (DMSO- d_6): δ (ppm) = 102.3 (OCH₂O), 107.1 (C α), 107.2 (C2), 109.3 (C5), 115.8 (CN), 121.0 (C2', C6'), 121.7 (C6), 124.6 (C4'), 125.8 (C γ), 129.2 (C3', C5'), 129.9 (C1), 138.8 (C1'), 148.1 (C δ), 148.8 (C3), 150.3 (C4), 152.6 (C β), 160.8 (CONH). EI/MS m/z (%): 318.1 (M^{•+}, 55), 226.1 (100), 196.0 (30), 159.0 (42), 140.0 (54).

(2E,4E)-5-(benzo[d][1,3]dioxol-5-yl)-N-benzyl-2-cyanopenta-2,4-dienamide (12). The crude product was purified by flash column chromatography (silica gel, dichloromethane). $\eta = 64\%$. ^1H NMR (DMSO- d_6): δ (ppm) = 4.39 (d, $J = 5.9$ Hz, 2H, NHCH₂Ph), 6.11 (s, 2H, OCH₂O), 6.99 (d, $J = 8.1$ Hz, 1H, H5), 7.06 (dd, $J = 11.5$ Hz, 15.2 Hz, 1H, H γ), 7.18 (dd, $J = 1.6$ Hz, 8.2 Hz, 1H, H6), 7.31 (m, 7H, H δ , H2, H2', H3', H4', H5', H6'), 7.96 (d, $J = 11.1$ Hz, 14.8 Hz, 1H, H β). 5.86 (t, $J = 5.9$ Hz, 1H, NH). ^{13}C NMR (DMSO- d_6): δ (ppm) = 43.4 (NHCH₂Ph), 102.2 (OCH₂O), 106.1 (C α), 107.1 (C2), 109.2 (C5), 116.0 (CN), 121.6 (C6), 125.6 (C γ), 127.4 (C4'), 127.8 (C2', C6'), 128.8 (C3', C5'), 129.9 (C1), 139.5 (C1'), 147.7 (C δ), 148.7 (C3), 150.1 (C4), 152.3 (C β), 161.5 (CONH). EI/MS m/z (%): 332.1 (M^{•+}, 100), 241.1 (65), 227.1 (54), 198.1 (32), 140.0 (61), 113.1 (19), 91.0 (98), 65.1 (20).

(2E,4E)-5-(benzo[d][1,3]dioxol-5-yl)-2-cyano-N-phenethylpenta-2,4-dienamide (13). The crude product was purified by flash column chromatography (silica gel, dichloromethane). $\eta = 87\%$. ^1H NMR (DMSO- d_6): δ (ppm) = 2.81 (m, 2H, NHCH₂CH₂Ph), 3.42 (dt, $J = 6.1$ Hz, 7.6 Hz, 2H, NHCH₂CH₂Ph), 6.11 (s, 2H, OCH₂O), 7.00 (d, $J = 8.1$ Hz, 1H, H5), 7.05 (dd, $J = 11.5$ Hz, 15.2 Hz, 1H, H γ), 7.19 (dd, $J = 1.6$ Hz, 8.3 Hz, 1H, H6), 7.22 (m, 3H, H2, H4', H δ), 7.32 (m, 2H, H2', H6'), 7.38 (m, 2H, H3', H5'), 7.90 (d, $J = 11.5$ Hz, 1H, H β), 8.36 (t, $J = 5.6$ Hz, 1H, NH). ^{13}C NMR (DMSO- d_6): δ (ppm) = 36.2 (NHCH₂CH₂Ph), 42.5 (NHCH₂CH₂Ph), 103.1 (OCH₂O), 107.1 (C α), 108.0 (C2), 110.1 (C5), 116.8 (CN), 122.5 (C6), 126.5 (C γ), 127.5 (C4'), 129.7 (C2', C6'), 130.0 (C3', C5'), 130.8 (C1), 140.6 (C1'), 148.4 (C β), 149.6 (C3), 151.0 (C4), 152.4 (C δ), 162.1 (CONH). EI/MS m/z (%): 346.1 (M^{•+}, 100), 241.1 (24), 226.1 (100), 196.0 (21), 159.0 (27), 140.0 (35).

4.1.3. General procedures for the synthesis of esters

4.1.3.1. Method A (Steglich esterification). To a stirred solution of piperic acid **2** (1 mmol) in dichloromethane, EDC.HCl (1.2 mmol) and DMAP (0.1 mmol) were added. The mixture was stirred at room temperature for 30 min. Then, the phenol (1.2 mmol) was added and the resulting mixture was stirred, protected from the light, overnight. Purification conditions are described in literature [21, 49].

Phenyl (2E,4E)-5-(benzo[d][1,3]dioxol-5-yl)penta-2,4-dienoate (6). Synthesis and structural analysis were previously reported [21].

Phenyl (2E,4E)-5-(benzo[d][1,3]dioxol-5-yl)-2-cyanopenta-2,4-dienoate (14). $\eta = 66$ %. ^1H NMR (CDCl_3-d_1): δ (ppm) = 6.06 (s, 2H, OCH_2O), 6.86 (d, $J = 8.0$ Hz, 1H, H5), 7.10 (dd, $J = 1.6$ Hz, 8.2 Hz, 1H, H6), 7.15 (d, $J = 1.6$ Hz, 1H, H2), 7.21 (m, 4H, H_γ , H δ , H2', H6'), 7.27 (m, 1H, H4') 7.42 (m, 2H, H3', H5'), 8.11 (d, $J = 11.0$ Hz, 1H, H β). ^{13}C NMR (CDCl_3-d_1): δ (ppm) = 102.0 (OCH_2O), 102.2 (C α), 106.8 (C2), 108.9 (C5), 114.6 (CN), 121.3 (C6), 121.3 (C2', C6'), 126.0 (C γ), 126.3 (C4'), 129.2 (C1), 129.6 (C3', C5'), 148.8 (C1'), 149.8 (C δ), 150.4 (C3), 150.9 (C4), 157.1 (C β), 161.3 (COO). EI/MS m/z (%): 319.0 (M^+ , 16), 226.0 (100), 196.0 (25), 159.0 (38), 140.0 (39).

Benzyl (2E,4E)-5-(benzo[d][1,3]dioxol-5-yl)-2-cyanopenta-2,4-dienoate (15). $\eta = 50$ %. ^1H NMR (CDCl_3-d_1): δ (ppm) = 5.31 (s, 2H, OCH_2Ph), 6.03 (s, 2H, OCH_2O), 6.84 (d, $J = 8.1$ Hz, 1H, H5), 7.06 (dd, $J = 1.6$ Hz, 8.2 Hz, 1H, H6), 7.14 (m, 3H, H_γ , H δ , H2), 7.38 (m, 5H, H2', H3', H4', H5', H6'), 7.99 (dd, $J = 10.9$ Hz, 1H, H β). ^{13}C NMR (CDCl_3-d_1): δ (ppm) = 67.6 (OCH_2Ph), 101.9 (OCH_2O), 102.9 (C α), 106.7 (C2), 108.8 (C5), 114.7 (CN), 121.3 (C6), 125.6 (C γ), 128.2 (C2', C6'), 128.5 (C4'), 128.7 (C3', C5'), 129.3 (C1), 135.1 (C1'), 148.7 (C3), 149.0 (C δ), 150.7 (C4), 156.0 (C β), 162.4 (COO). EI/MS m/z (%): 333.1 (M^+ , 19), 242.0 (29), 175.0 (25), 91.0 (100).

Phenethyl (2E,4E)-5-(benzo[d][1,3]dioxol-5-yl)-2-cyanopenta-2,4-dienoate (16). $\eta = 51$ %. ^1H NMR (CDCl_3-d_1): δ (ppm) = 3.04 (t, $J = 7.0$ Hz, 2H, $\text{OCH}_2\text{CH}_2\text{Ph}$), 4.46 (t, $J = 7.1$ Hz, 2H, $\text{OCH}_2\text{CH}_2\text{Ph}$), 6.04 (s, 2H, OCH_2O), 6.84 (d, $J = 8.0$ Hz, 1H, H5), 7.11 (m, 4H, H6, H2, H δ , H_γ), 7.15 (m, 3H, H2', H4', H6'), 7.33 (m, 2H, H3', H5'), 7.92 (d, $J = 10.9$ Hz, 1H, H β). ^{13}C NMR (CDCl_3-d_1): δ (ppm) = 35.1 ($\text{OCH}_2\text{CH}_2\text{Ph}$), 66.6 ($\text{OCH}_2\text{CH}_2\text{Ph}$), 101.9 (OCH_2O), 102.9 (C α), 106.7 (C2), 108.8 (C5), 114.7 (CN), 121.3 (C6), 125.6 (C γ), 126.8 (C4'), 128.6 (C2', C6'), 129.1 (C3', C5'), 129.3 (C1), 137.3 (C1'), 148.7 (C3), 148.8 (C δ), 150.6 (C4), 155.7 (C β), 162.5 (COO). EI/MS m/z (%): 347.1 (M^+ , 34), 243.1 (21), 198.1 (31), 140.0 (37), 105.1 (100).

4.1.3.2. Method B (bimolecular nucleophilic substitution). Piperic acid **2** (1 mmol) was dissolved in DMF and K_2CO_3 (1.2 mmol) was added. The mixture was stirred at room temperature for 30 min. Then, the appropriate alkyl bromide (benzyl bromide or (2-bromoethyl)benzene) (1.2 mmol) was added and the mixture was stirred, protected from the light, at 80 °C for 8 h. Purification conditions are described in literature [21, 50].

Benzyl (2E,4E)-5-(benzo[d][1,3]dioxol-5-yl)penta-2,4-dienoate (7). Synthesis and structural analysis were previously reported [21].

Phenethyl (2E,4E)-5-(benzo[d][1,3]dioxol-5-yl)penta-2,4-dienoate (8). $\eta = 84\%$. $^1\text{H NMR}$ (CDCl_3-d_1): δ (ppm) = 2.99 (*t*, $J = 7.1$ Hz, 2H, $\text{OCH}_2\text{CH}_2\text{Ph}$), 4.38 (*t*, $J = 7.1$ Hz, 2H, $\text{OCH}_2\text{CH}_2\text{Ph}$), 5.93 (*d*, $J = 15.3$ Hz, 1H, $\text{H}\alpha$), 5.98 (*s*, 2H, OCH_2O), 6.79 (*dd*, $J = 10.8$ Hz, 15.5 Hz, 1H, $\text{H}\gamma$), 6.79 (*m*, 2H, H_5 , $\text{H}\delta$), 6.91 (*dd*, $J = 1.6$ Hz, 8.2 Hz, 1H, H_6), 6.99 (*d*, $J = 1.6$ Hz, 1H, H_2), 7.23 (*m*, 3H, H_2' , H_4' , H_6'), 7.32 (*m*, 2H, H_3' , H_5'), 7.39 (*dd*, $J = 10.7$ Hz, 15.2 Hz, 1H, $\text{H}\beta$). $^{13}\text{C NMR}$ (CDCl_3-d_1): δ (ppm) = 35.2 ($\text{OCH}_2\text{CH}_2\text{Ph}$), 64.8 ($\text{OCH}_2\text{CH}_2\text{Ph}$), 101.4 (OCH_2O), 105.9 (C2), 108.6 (C5), 120.2 (C α), 123.0 (C6), 124.5 (C γ), 126.5 (C4'), 128.5 (C2', C6'), 128.9 (C3', C5'), 130.6 (C1), 138.0 (C1'), 140.2 (C δ), 144.9 (C β), 148.3 (C3), 148.6 (C4), 167.0 (COO). EI/MS m/z (%): 322.1 (M^{*+} , 65), 218.2 (17), 173.1 (100), 143.1 (38), 115.1 (94), 91.2 (20), 77.2 (19), 65.2 (18).

4.1.4. Synthesis of (E)-3-(benzo[d][1,3]dioxol-5-yl)acrylate (18). Aldehyde **17** (1 mmol) dissolved in anhydrous pyridine. Then, mono-ethyl malonate (1.5 mmol) and piperidine (0.35 mmol) were added. The mixture was heated until the maximum aldehyde consumption was observed by TLC. Once the reaction was complete, the product was purified by column chromatography (silica gel, dichloromethane). The procedure was adapted from Teixeira *et al.* [51] with some modifications. $\eta = 91\%$. $^1\text{H NMR}$ (CDCl_3-d_1): δ (ppm) = 1.33 (*t*, $J = 7.1$ Hz, 3H, OCH_2CH_3), 4.25 (*q*, $J = 7.1$ Hz, 2H, OCH_2CH_3), 6.00 (*s*, 2H, OCH_2O), 6.26 (*d*, $J = 15.9$ Hz, 1H, $\text{H}\alpha$), 6.81 (*d*, $J = 8.0$ Hz, 1H, H_5), 7.00 (*dd*, $J = 1.5$ Hz, 8.1 Hz, 1H, H_6), 7.03 (*d*, $J = 1.7$ Hz, 1H, H_2), 7.59 (*d*, $J = 15.9$ Hz, 1H, $\text{H}\beta$). $^{13}\text{C NMR}$ (CDCl_3-d_1): δ (ppm) = 14.4 (OCH_2CH_3), 60.4 (OCH_2CH_3), 101.5 (OCH_2O), 106.5 (C2), 108.5 (C5), 116.3 (C α), 124.4 (C6), 128.9 (C1), 144.3 (C β), 148.3 (C3), 149.6 (C4), 167.2 (COO). EI/MS m/z (%): 220.2 (M^{*+} , 100), 175.1 (58), 117.0 (31), 89.0 (64), 63.1 (41).

4.1.5. Synthesis of (E)-3-(benzo[d][1,3]dioxol-5-yl)prop-2-en-1-ol (19). Cinnamic ester **18** (1 mmol) was dissolved in dry THF under argon atmosphere and cooled to -78 °C. Then, LiAlH_4 (1.5 mmol) was added, and the mixture was stirred for 5 h. Once the reaction was complete, the unreacted LiAlH_4 was quenched with methanol until gas evolution stopped, and water (60 mL) was added. The mixture was neutralized with HCl 6 M, then extracted with dichloromethane (3×30 mL). The combined organic layer was washed with brine (20 mL), dried over anhydrous sodium sulfate, filtered and concentrated. Purification by flash column chromatography (silica gel, dichloromethane) yielded the cinnamyl alcohols **19**. The procedure was adapted from Jirásek *et al.* [52] with some modifications. $\eta = 43\%$. $^1\text{H NMR}$ (CDCl_3-d_1): δ (ppm) = 4.29 (*dd*, $J = 0.9$ Hz, 5.8 Hz, 2H, CH_2OH), 5.95 (*s*, 2H, OCH_2O), 6.19 (*d*, $J = 5.9$ Hz, 15.8 Hz, 1H, $\text{H}\alpha$), 6.52 (*d*, $J = 15.8$ Hz, 1H, $\text{H}\beta$), 6.75 (*d*, $J = 8.0$ Hz, 1H, H_5), 6.81 (*dd*, $J = 1.6$ Hz, 8.1 Hz, 1H, H_6), 6.93 (*d*, $J = 1.7$ Hz, 1H, H_2). $^{13}\text{C NMR}$ (CDCl_3-d_1): δ (ppm) = 63.8 (CH_2OH), 101.1 (OCH_2O), 105.8 (C2), 108.3 (C5), 121.2 (C6), 126.7 (C α), 131.0 (C β), 131.2 (C1), 147.3 (C3), 148.0 (C4). EI/MS m/z (%): 178.2 (M^{*+} , 80), 135.1 (100), 122.1 (42), 91.1 (24).

4.1.6. Synthesis of (*E*)-3-(benzo[*d*][1,3]dioxol-5-yl)acrylaldehyde (20). Cinnamyl alcohol **19** (1 mmol) was dissolved in dichloromethane, and MnO₂ (9 mmol) was added. The mixture was stirred overnight at room temperature. Then, the mixture was filtered through celite to remove the MnO₂ and washed with dichloromethane. The filtrate was concentrated and purified by flash column chromatography (silica gel, dichloromethane). The procedure was adapted from Jirásek *et al.* [52] with some modifications. $\eta = 62\%$. ¹H NMR (CDCl₃-*d*₁): δ (ppm) = 6.04 (*s*, 2H, OCH₂O), 6.56 (*dd*, *J* = 7.7 Hz, 15.8 Hz, 1H, H α), 6.86 (*d*, *J* = 8.5 Hz, 1H, H5), 7.07 (*m*, 2H, H2, H6), 7.38 (*d*, *J* = 15.8 Hz, 1H, H β), 9.05 (*d*, *J* = 7.7 Hz, 1H, CHO). ¹³C NMR (CDCl₃-*d*₁): δ (ppm) = 101.8 (OCH₂O), 106.8 (C2), 108.8 (C5), 125.3 (C α), 126.9 (C6), 128.5 (C1), 148.6 (C3), 150.5 (C4), 152.5 (C β), 193.5 (CHO). EI/MS *m/z* (%): 176.1 (M⁺, 100), 147.1 (67), 118.1 (48), 89.2 (88), 63.1 (74), 51.1 (20).

4.1.7. Synthesis of (2*E*,4*E*)-5-(benzo[*d*][1,3]dioxol-5-yl)-2-cyanopenta-2,4-dienoic acid (9). Aldehyde **20** (1 mmol) was dissolved in anhydrous pyridine. Then, cyanoacetic acid (1.5 mmol) and piperidine (0.35 mmol) were added. The mixture was heated until the maximum aldehyde consumption was observed by TLC. Upon completion, the reaction mixture was acidified with HCl 6 M and the solid formed was isolated by filtration under reduced pressure. The procedure was adapted from Teixeira *et al.* [51] with some modifications. $\eta = 87\%$. ¹H NMR (DMSO-*d*₆): δ (ppm) = 6.12 (*s*, 2H, OCH₂O), 7.01 (*d*, *J* = 8.0 Hz, 1H, H5), 7.08 (*dd*, *J* = 11.7 Hz, 15.0 Hz, 1H, H γ), 7.19 (*dd*, *J* = 1.4 Hz, 8.1 Hz, 1H, H6), 7.41 (*m*, 1H, H2), 7.56 (*d*, *J* = 15.1 Hz, 1H, H δ), 8.03 (*d*, *J* = 11.6 Hz, 1H, H β), 13.6 (*bs*, 1H, COOH). ¹³C NMR (DMSO-*d*₆): δ (ppm) = 103.2 (OCH₂O), 104.3 (C α), 108.1 (C2), 110.2 (C5), 116.6 (CN), 122.3 (C6), 127.2 (C γ), 130.7 (C1), 149.7 (C3), 150.8 (C β), 151.4 (C4), 157.0 (C δ), 164.8 (COOH). EI/MS *m/z* (%): 243.2 (M⁺, 27), 198.2 (34), 140.1 (100), 113.1 (24).

4.2. Enzymatic assays

4.2.1. Evaluation of human monoamine oxidase (hMAO) inhibitory activity

The inhibitory activity of piperine and the derivatives thereof on hMAO-A and hMAO-B was studied using an experimental protocol described elsewhere [21, 22] (see supplementary information).

4.2.2. Evaluation of human monoamine oxidases kinetics and human monoamine oxidase-B-inhibitor kinetics

To determine the steady-state kinetic parameters (*K*_m, Michaelis constant, and *V*_{max}, maximum velocity) of hMAO-A and hMAO-B, the enzymatic activity of both isoforms was studied in the presence six different concentrations of kynuramine (see SI). To evaluate the mechanism of hMAO-B inhibition of compounds **7**, **10** and **15**, substrate-dependent kinetic experiments were also performed (see supplementary information).

4.3. *In vitro* toxicology

4.3.1. Cell lines and culture conditions

Human SH-SY5Y neuroblastoma cells and human epithelial colorectal adenocarcinoma (Caco-2) cells were obtained from the American Type Culture Collection (ATCC, Manassas, VA, USA). Cell

cultures and SH-SY5Y cell differentiation were performed as previously described by Fernandes *et al.* [53] and in supplementary information.

4.3.2. Evaluation of cytotoxicity profile

Stock solutions of the test compounds (100 mM) were freshly prepared in DMSO. Final concentrations of the test compounds were obtained by diluting into culture medium immediately before use, giving a final maximum concentration of 0.1 % DMSO.

In cytotoxicity studies, differentiated SH-SY5Y cells were exposed to the test compounds (10 μ M and 50 μ M) for 24 h. Controls were treated with culture media containing 0.1 % DMSO. Cell viability was estimated using two different methods: resazurin reduction assay and NR uptake assay. The cytotoxicity end-points were performed as described in literature [40, 53] and in supplementary information.

4.3.3. Evaluation of intracellular oxidative stress levels

The formation of intracellular RS was evaluated using the 2',7'-dichlorofluorescein (DCF) fluorescence assay as previously described by da Fernandes *et al.* [53] and in supplementary information.

4.3.4. Evaluation of P-glycoprotein (P-gp) transport activity

The effects of the tested compounds on P-gp transport activity was evaluated using rhodamine 123 (RHO 123) as a P-gp fluorescent substrate in Caco-2 cells as previously described by Fernandes *et al.* [40] and in supplementary information.

4.4. Statistical analysis

Data analysis for all the studies are specified in supplementary information.

4.5. Evaluation of the chromatographic hydrophobicity index

Chromatographic hydrophobicity index $\log D$ at pH 7.4 (CHI $\log D_{7.4}$) values were determined using an experimental protocol described elsewhere [43, 54]. Chromatographic hydrophobicity index $\log D$ at pH 7.4 (CHI $\log D_{7.4}$) values were determined using the retention times of samples and a mixture of standard compounds. The data was acquired on a Shimadzu high-performance liquid chromatograph SPD-M20A system (Shimadzu, Kyoto, Japan) with a Luna C18 (2) column (Phenomenex, CA, USA) 150 \times 4.6 mm, 5 μ m. The mobile phase A was 10 mM ammonium acetate solution (pH 7.4), and mobile phase B was acetonitrile. The following gradient program was applied: 1 mL/min flow, rt, injection volume 20 μ L, gradient 0–6 min 0-100 % B, 6–14 min 100% B, 14–16 min 100-0 % B.

A calibration plot was obtained using a mixture of the following compounds: paracetamol, theophylline, caffeine, benzimidazole, colchicine, carbamazepine, indole, propiophenone, butyrophenone, valerophenone, and heptanophenone (see supplementary information, **Figure S1** and **Table S1**). Stock solutions of the test compounds (10 μ M) were prepared in DMSO and diluted in acetonitrile/water (1:1) to obtain a final concentration of 250 μ M. CHI $\log D_{7.4}$ values were calculated as previously described [43, 54].

4.6. Estimation of drug-like properties

The calculation of molecular weight (MW), topological polar surface area (TPSA), number of hydrogen bond donors (HBD) and acceptors (HBA), number of rotatable bonds (RB) and logarithm of the ratio of the concentration of a drug in the brain and in the blood (logBB) was performed using the StarDrop software.

5. Acknowledgements

This project was supported by Foundation for Science and Technology (FCT) and FEDER/COMPETE research grants (UID/QUI/00081, NORTE-01-0145-FEDER-000028, POCI-01-0145-FEDER-029164). D. Chavarría, C. Fernandes, E. Martins, V. Silva, C. Silva, P. Soares and T. Silva grants are supported by FCT, POPH and FEDER/COMPETE and NORTE-01-0145-FEDER-000028. This article is based upon work from COST Action CA15135.

6. References

- [1] M. Goedert, Alzheimer's and Parkinson's diseases: The prion concept in relation to assembled A β , tau, and α -synuclein, *Science*, 349 (2015) 1255555. <https://doi.org/10.1126/science.1255555>
- [2] Y. He, Z. Yu, S. Chen, Alpha-Synuclein Nitration and Its Implications in Parkinson's Disease, *ACS Chem. Neurosci.*, 10 (2019) 777-782. <https://doi.org/10.1021/acscemneuro.8b00288>
- [3] B.C. Shook, P.F. Jackson, Adenosine A_{2A} Receptor Antagonists and Parkinson's Disease, *ACS Chem. Neurosci.*, 2 (2011) 555-567. <https://doi.org/10.1021/cn2000537>
- [4] Y.D. Wang, X.Q. Bao, S. Xu, W.W. Yu, S.N. Cao, J.P. Hu, Y. Li, X.L. Wang, D. Zhang, S.S. Yu, A Novel Parkinson's Disease Drug Candidate with Potent Anti-neuroinflammatory Effects through the Src Signaling Pathway, *J. Med. Chem.*, 59 (2016) 9062-9079. <https://doi.org/10.1021/acs.jmedchem.6b00976>
- [5] L.V. Kalia, A.E. Lang, Parkinson's disease, *Lancet*, 386 (2015) 896-912. [https://doi.org/10.1016/s0140-6736\(14\)61393-3](https://doi.org/10.1016/s0140-6736(14)61393-3)
- [6] S.F. Graham, N.L. Rey, A. Yilmaz, P. Kumar, Z. Madaj, M. Maddens, R.O. Bahado-Singh, K. Becker, E. Schulz, L.K. Meyerdirk, J.A. Steiner, J. Ma, P. Brundin, Biochemical Profiling of the Brain and Blood Metabolome in a Mouse Model of Prodromal Parkinson's Disease Reveals Distinct Metabolic Profiles, *J. Proteome Res.*, 17 (2018) 2460-2469. <https://doi.org/10.1021/acs.jproteome.8b00224>
- [7] J. Zheng, X. Zhang, X. Zhen, Development of Adenosine A_{2A} Receptor Antagonists for the Treatment of Parkinson's Disease: A Recent Update and Challenge, *ACS Chem. Neurosci.*, 10 (2019) 783-791. <https://doi.org/10.1021/acscemneuro.8b00313>
- [8] C. Binda, P. Newton-Vinson, F. Hubalek, D.E. Edmondson, A. Mattevi, Structure of human monoamine oxidase B, a drug target for the treatment of neurological disorders, *Nat. Struct. Biol.*, 9 (2002) 22-26. <https://doi.org/10.1038/nsb732>
- [9] C. Binda, J. Wang, L. Pisani, C. Caccia, A. Carotti, P. Salvati, D.E. Edmondson, A. Mattevi, Structures of human monoamine oxidase B complexes with selective noncovalent inhibitors: safinamide and coumarin analogs, *J. Med. Chem.*, 50 (2007) 5848-5852. <https://doi.org/10.1021/jm070677y>

- [10] H.P. Booyesen, C. Moraal, G. Terre'Blanche, A. Petzer, J.J. Bergh, J.P. Petzer, Thio- and aminocaffeine analogues as inhibitors of human monoamine oxidase, *Bioorg. Med. Chem.*, 19 (2011) 7507-7518. <https://doi.org/10.1016/j.bmc.2011.10.036>
- [11] N.M. Malek, D.G. Grosset, Investigational agents in the treatment of Parkinson's disease: focus on safinamide, *J. Exp. Pharmacol.*, 4 (2012) 85-90. <https://doi.org/10.2147/JEP.S34343>
- [12] A. Stöbel, M. Schlenk, S. Hinz, P. Küppers, J. Heer, M. Gütschow, C.E. Müller, Dual targeting of adenosine A_{2A} receptors and monoamine oxidase B by 4*H*-3,1-benzothiazin-4-ones, *J. Med. Chem.*, 56 (2013) 4580-4596. <https://doi.org/10.1021/jm400336x>
- [13] H.A. Blair, S. Dhillon, Safinamide: A Review in Parkinson's Disease, *CNS Drugs*, 31 (2017) 169-176. <https://doi.org/10.1007/s40263-017-0408-1>
- [14] D. Robakis, S. Fahn, Defining the Role of the Monoamine Oxidase-B Inhibitors for Parkinson's Disease, *CNS Drugs*, 29 (2015) 433-441. <https://doi.org/10.1007/s40263-015-0249-8>
- [15] J. Wattanathorn, P. Chonpathompikunlert, S. Muchimapura, A. Priprem, O. Tankamerdthai, Piperine, the potential functional food for mood and cognitive disorders, *Food Chem. Toxicol.*, 46 (2008) 3106-3110. <https://doi.org/10.1016/j.fct.2008.06.014>
- [16] Q.Q. Mao, Z. Huang, S.P. Ip, Y.F. Xian, C.T. Che, Protective effects of piperine against corticosterone-induced neurotoxicity in PC12 cells, *Cell. Mol. Neurobiol.*, 32 (2012) 531-537. <https://doi.org/10.1007/s10571-011-9786-y>
- [17] W. Yang, Y.H. Chen, H. Liu, H.D. Qu, Neuroprotective effects of piperine on the 1-methyl-4-phenyl-1,2,3,6-tetrahydropyridine-induced Parkinson's disease mouse model, *Int. J. Mol. Med.*, 36 (2015) 1369-1376. <https://doi.org/10.3892/ijmm.2015.2356>
- [18] P. Shrivastava, K. Vaibhav, R. Tabassum, A. Khan, T. Ishrat, M.M. Khan, A. Ahmad, F. Islam, M.M. Safhi, F. Islam, Anti-apoptotic and Anti-inflammatory effect of Piperine on 6-OHDA induced Parkinson's Rat model, *J. Nutr. Biochem.*, 24 (2013) 680-687. <https://doi.org/10.1016/j.jnutbio.2012.03.018>
- [19] Y. Bi, P.C. Qu, Q.S. Wang, L. Zheng, H.L. Liu, R. Luo, X.Q. Chen, Y.Y. Ba, X. Wu, H. Yang, Neuroprotective effects of alkaloids from Piper longum in a MPTP-induced mouse model of Parkinson's disease, *Pharm. Biol.*, 53 (2015) 1516-1524. <https://doi.org/10.3109/13880209.2014.991835>
- [20] S.A. Lee, S.S. Hong, X.H. Han, J.S. Hwang, G.J. Oh, K.S. Lee, M.K. Lee, B.Y. Hwang, J.S. Ro, Piperine from the fruits of Piper longum with inhibitory effect on monoamine oxidase and antidepressant-like activity, *Chem. Pharm. Bull. (Tokyo)*, 53 (2005) 832-835. <https://doi.org/10.1248/cpb.53.832>
- [21] D. Chavarria, F. Cagide, M. Pinto, L.R. Gomes, J.N. Low, F. Borges, Development of piperic acid-based monoamine oxidase inhibitors: Synthesis, structural characterization and biological evaluation, *J. Mol. Struct.*, 1182 (2019) 298-307. <https://doi.org/10.1016/j.molstruc.2019.01.060>
- [22] S. Hagenow, A. Stasiak, R.R. Ramsay, H. Stark, Ciproxifan, a histamine H₃ receptor antagonist, reversibly inhibits monoamine oxidase A and B, *Sci. Rep.*, 7 (2017) 1-6. <https://doi.org/10.1038/srep40541>
- [23] Y.T. Cheung, W.K. Lau, M.S. Yu, C.S. Lai, S.C. Yeung, K.F. So, R.C. Chang, Effects of all-*trans*-retinoic acid on human SH-SY5Y neuroblastoma as in vitro model in neurotoxicity research, *Neurotoxicology*, 30 (2009) 127-135. <https://doi.org/10.1016/j.neuro.2008.11.001>

- [24] Z. Ujhelyi, F. Fenyvesi, J. Varadi, P. Feher, T. Kiss, S. Veszeka, M. Deli, M. Vecsernyes, I. Bacskay, Evaluation of cytotoxicity of surfactants used in self-micro emulsifying drug delivery systems and their effects on paracellular transport in Caco-2 cell monolayer, *Eur. J. Pharm. Sci.*, 47 (2012) 564-573. <https://doi.org/10.1016/j.ejps.2012.07.005>
- [25] J. Kovalevich, D. Langford, Considerations for the Use of SH-SY5Y Neuroblastoma Cells in Neurobiology, *Methods Mol. Biol.*, 1078 (2013) 9-21. https://doi.org/10.1007/978-1-62703-640-5_2
- [26] F.M. Lopes, R. Schroder, M.L. da Frota, Jr., A. Zanotto-Filho, C.B. Muller, A.S. Pires, R.T. Meurer, G.D. Colpo, D.P. Gelain, F. Kapczinski, J.C. Moreira, C. Fernandes Mda, F. Klamt, Comparison between proliferative and neuron-like SH-SY5Y cells as an in vitro model for Parkinson disease studies, *Brain Res.*, 1337 (2010) 85-94. <https://doi.org/10.1016/j.brainres.2010.03.102>
- [27] F.M. Lopes, G.F. Londero, L.M. de Medeiros, L.L. da Motta, G.A. Behr, V.A. de Oliveira, M. Ibrahim, J.C. Moreira, L.O. Porciuncula, J.B. da Rocha, F. Klamt, Evaluation of the neurotoxic/neuroprotective role of organoselenides using differentiated human neuroblastoma SH-SY5Y cell line challenged with 6-hydroxydopamine, *Neurotox. Res.*, 22 (2012) 138-149. <https://doi.org/10.1007/s12640-012-9311-1>
- [28] F.S. Silva, I.G. Starostina, V.V. Ivanova, A.A. Rizvanov, P.J. Oliveira, S.P. Pereira, Determination of Metabolic Viability and Cell Mass Using a Tandem Resazurin/Sulforhodamine B Assay, *Curr. Protoc. Toxicol.*, 68 (2016) 2.24.21-22.24.15. <https://doi.org/10.1002/cptx.1>
- [29] G. Repetto, A. del Peso, J.L. Zurita, Neutral red uptake assay for the estimation of cell viability/cytotoxicity, *Nat. Protoc.*, 3 (2008) 1125-1131. <https://doi.org/10.1038/nprot.2008.75>
- [30] J.P. Kehrer, L.O. Klotz, Free radicals and related reactive species as mediators of tissue injury and disease: implications for Health, *Crit. Rev. Toxicol.*, 45 (2015) 765-798. <https://doi.org/10.3109/10408444.2015.1074159>
- [31] Q. Liu, J. Hou, X. Chen, G. Liu, D. Zhang, H. Sun, J. Zhang, P-glycoprotein mediated efflux limits the transport of the novel anti-Parkinson's disease candidate drug FLZ across the physiological and PD pathological in vitro BBB models, *PLoS One*, 9 (2014) e102442. <https://doi.org/10.1371/journal.pone.0102442>
- [32] L. Partridge, Intervening in ageing to prevent the diseases of ageing, *Trends Endocrinol. Metab.*, 25 (2014) 555-557. <https://doi.org/10.1016/j.tem.2014.08.003>
- [33] D.S. Miller, B. Bauer, A.M.S. Hartz, Modulation of P-glycoprotein at the blood-brain barrier: opportunities to improve central nervous system pharmacotherapy, *Pharmacol. Rev.*, 60 (2008) 196-209. <https://doi.org/10.1124/pr.107.07109>
- [34] F. Faassen, G. Vogel, H. Spanings, H. Vromans, Caco-2 permeability, P-glycoprotein transport ratios and brain penetration of heterocyclic drugs, *Int. J. Pharm.*, 263 (2003) 113-122. [https://doi.org/10.1016/S0378-5173\(03\)00372-7](https://doi.org/10.1016/S0378-5173(03)00372-7)
- [35] R. Silva, H. Carmo, R. Dinis-Oliveira, A. Cordeiro-da-Silva, S.C. Lima, F. Carvalho, L. Bastos Mde, F. Remiao, *In vitro* study of P-glycoprotein induction as an antidotal pathway to prevent cytotoxicity in Caco-2 cells, *Arch. Toxicol.*, 85 (2011) 315-326. <https://doi.org/10.1007/s00204-010-0587-8>
- [36] M. Gameiro, R. Silva, C. Rocha-Pereira, H. Carmo, F. Carvalho, M.L. Bastos, F. Remiao, Cellular Models and *In Vitro* Assays for the Screening of modulators of P-gp, MRP1 and BCRP, *Molecules: a*

- journal of synthetic chemistry and natural product chemistry., 22 (2017) 1-48.
<https://doi.org/10.3390/molecules22040600>
- [37] J.J. Hakkarainen, A.J. Jalkanen, T.M. Kaariainen, P. Keski-Rahkonen, T. Venalainen, J. Hokkanen, J. Monkkonen, M. Suhonen, M.M. Forsberg, Comparison of *in vitro* cell models in predicting *in vivo* brain entry of drugs, *Int. J. Pharm.*, 402 (2010) 27-36. <https://doi.org/10.1016/j.ijpharm.2010.09.016>
- [38] E. Hellinger, S. Veszeka, A.E. Toth, F. Walter, A. Kittel, M.L. Bakk, K. Tihanyi, V. Hada, S. Nakagawa, T.D. Duy, M. Niwa, M.A. Deli, M. Vastag, Comparison of brain capillary endothelial cell-based and epithelial (MDCK-MDR1, Caco-2, and VB-Caco-2) cell-based surrogate blood-brain barrier penetration models, *Eur. J. Pharm. Sci.*, 82 (2012) 340-351. <https://doi.org/10.1016/j.ejpb.2012.07.020>
- [39] D.B. Stanimirovic, M. Bani-Yaghoub, M. Perkins, A.S. Haqqani, Blood-brain barrier models: *in vitro* to *in vivo* translation in preclinical development of CNS-targeting biotherapeutics, *Expert Opin. Drug Discov.*, 10 (2015) 141-155. <https://doi.org/10.1517/17460441.2015.974545>
- [40] C. Fernandes, C. Martins, A. Fonseca, R. Nunes, M.J. Matos, R. Silva, J. Garrido, B. Sarmento, F. Remiao, F.J. Otero-Espinar, E. Uriarte, F. Borges, PEGylated PLGA Nanoparticles As a Smart Carrier to Increase the Cellular Uptake of a Coumarin-Based Monoamine Oxidase B Inhibitor, *ACS Appl. Mater. Interfaces*, 10 (2018) 39557-39569. <https://doi.org/10.1021/acsami.8b17224>
- [41] A.L. Bartels, Blood-brain barrier P-glycoprotein function in neurodegenerative disease, *Curr. Pharm. Des.*, 17 (2011) 2771-2777. <https://doi.org/10.2174/138161211797440122>
- [42] T. Müller, ABCB1: is there a role in the drug treatment of Parkinson's disease?, *Expert Opin. Drug Metab. Toxicol.*, 14 (2018) 127-129. <https://doi.org/10.1080/17425255.2018.1416096>
- [43] G. Camurri, A. Zaramella, High-throughput liquid chromatography/mass spectrometry method for the determination of the chromatographic hydrophobicity index, *Anal. Chem.*, 73 (2001) 3716-3722. <https://doi.org/10.1021/ac001388j>
- [44] K. Valko, C. Bevan, D. Reynolds, Chromatographic Hydrophobicity Index by Fast-Gradient RP-HPLC: A High-Throughput Alternative to log P/log D, *Anal. Chem.*, 69 (1997) 2022-2029. <https://doi.org/10.1021/ac961242d>
- [45] D.E. Clark, Rapid calculation of polar molecular surface area and its application to the prediction of transport phenomena. 2. Prediction of blood-brain barrier penetration, *J. Pharm. Sci.*, 88 (1999) 815-821. <https://doi.org/10.1021/js980402t>
- [46] S.A. Hitchcock, L.D. Pennington, Structure-brain exposure relationships, *J. Med. Chem.*, 49 (2006) 7559-7583. <https://doi.org/10.1021/jm060642i>
- [47] H. Pajouhesh, G.R. Lenz, Medicinal Chemical Properties of Successful Central Nervous System Drugs, *NeuroRx.*, 2 (2005) 541-553. <https://doi.org/10.1602/neurorx.2.4.541>
- [48] A. Gaspar, T. Silva, M. Yanez, D. Vina, F. Orallo, F. Ortuso, E. Uriarte, S. Alcaro, F. Borges, Chromone, a privileged scaffold for the development of monoamine oxidase inhibitors, *J. Med. Chem.*, 54 (2011) 5165-5173. <https://doi.org/10.1021/jm2004267>
- [49] M. Soda, D. Hu, S. Endo, M. Takemura, J. Li, R. Wada, S. Ifuku, H.T. Zhao, O. El-Kabbani, S. Ohta, K. Yamamura, N. Toyooka, A. Hara, T. Matsunaga, Design, synthesis and evaluation of caffeic acid phenethyl ester-based inhibitors targeting a selectivity pocket in the active site of human aldo-keto reductase 1B10, *Eur. J. Med. Chem.*, 48 (2012) 321-329. <https://doi.org/10.1016/j.ejmech.2011.12.034>

- [50] H. Shi, D. Xie, R. Yang, Y. Cheng, Synthesis of caffeic acid phenethyl ester derivatives, and their cytoprotective and neuritogenic activities in PC12 cells, *J. Agric. Food Chem.*, 62 (2014) 5046-5053. <https://doi.org/10.1021/jf500464k>
- [51] J. Teixeira, T. Silva, S. Benfeito, A. Gaspar, E.M. Garrido, J. Garrido, F. Borges, Exploring nature profits: development of novel and potent lipophilic antioxidants based on galloyl-cinnamic hybrids, *Eur. J. Med. Chem.*, 62 (2013) 289-296. <https://doi.org/10.1016/j.ejmech.2012.12.049>
- [52] P. Jirasek, S. Amslinger, J. Heilmann, Synthesis of natural and non-natural curcuminoids and their neuroprotective activity against glutamate-induced oxidative stress in HT-22 cells, *J. Nat. Prod.*, 77 (2014) 2206-2217. <https://doi.org/10.1021/np500396y>
- [53] C. Fernandes, M. Pinto, C. Martins, M.J. Gomes, B. Sarmiento, P.J. Oliveira, F. Remião, F. Borges, Development of a PEGylated-Based Platform for Efficient Delivery of Dietary Antioxidants Across the Blood-Brain Barrier, *Bioconjug. Chem.*, 29 (2018) 1677-1689. <https://doi.org/10.1021/acs.bioconjchem.8b00151>
- [54] K. Valko, S. Nunhuck, C. Bevan, M.H. Abraham, D.P. Reynolds, Fast gradient HPLC method to determine compounds binding to human serum albumin. Relationships with octanol/water and immobilized artificial membrane lipophilicity, *J. Pharm. Sci.*, 92 (2003) 2236-2248. <https://doi.org/10.1002/jps.10494>